

Broadband extraordinary optical transmission through tapered metallic slits array embedded with rectangular cavities

Qi Yunping¹, Zhang Xuwei¹, Hu Yue¹, Hu Binbing¹, Wang Xiangxian²

(1. College of Physics and Electronic Engineering, Northwest Normal University, Lanzhou 730070, China;

(2. School of Science, Lanzhou University of Technology, Lanzhou 730050, China)

Abstract: To achieve nonresonant broadband extraordinary optical transmission (EOT), tapered metallic slits array embedded with rectangular cavities structure was proposed and its transmission properties were investigated using the finite element method (FEM). The results show that tapered metallic slits array embedded with rectangular cavities can achieve broadband and wide-angle enhanced transmission in the infrared and the light is strongly localized enhanced at the slit exits, in contrast with straight slits structure. The phenomenon was described with a transmission line model. In addition, the effects of incident polarization, the entrance width of the slit, and the centers misalignment of the tapered slits on the transmission property were also studied. These results would be helpful for optical signal transmission and the designing near field light harvesting devices with broadband and strong transmission.

Key words: extraordinary optical transmission; surface plasmon polaritons; tapered metallic slits array; the finite element method

CLC number: O436 **Document code:** A **DOI:** 10.3788/IRLA201847.S107001

内嵌矩形腔楔形金属狭缝阵列的宽频异常透射

祁云平¹, 张雪伟¹, 胡月¹, 胡兵兵¹, 王向贤²

(1. 西北师范大学物理与电子工程学院, 甘肃兰州 730070;

2. 兰州理工大学理学院, 甘肃兰州 730050)

摘要: 为了实现宽频透射, 设计了内嵌矩形腔的楔形金属狭缝结构, 并用有限元方法研究了其透射特性。结果表明, 内嵌矩形腔的楔形金属狭缝阵列在红外范围内可以实现宽带、广角度的增强传输, 并且与直缝结构对比光是强烈局域在狭缝出口处。用传输线理论来描述这种现象。此外, 还讨论了入射极化角度、狭缝入口宽度、楔形狭缝的中心偏置等因素对透射的影响。这些结果对光信号传输、宽带传输和近场光采集装置的设计具有一定的指导意义。

关键词: 光学异常透射; 表面等离子激元; 楔形金属狭缝; 有限元法

收稿日期: 2018-02-23; 修订日期: 2018-04-16

基金项目: 国家自然科学基金(61367005, 61741119); 甘肃省自然科学基金(17JR5RA078);

西北师范大学“学生创新能力提升计划”(CX2018Y167)

作者简介: 祁云平(1981-), 男, 副教授, 硕士生导师, 博士, 主要从事表面等离子激元纳米光子学方面的研究。Email: yunpqi@126.com

0 Introduction

The extraordinary optical transmission (EOT) phenomenon was observed in an opaque metallic film with a periodic array of subwavelength holes in 1998^[1]. Many EOT phenomena based on metal nanostructures have been investigated theoretically and experimentally, which would provide potential applications in integrated optoelectronic devices, such as nonlinear optics, and surface enhanced Raman scattering, et al^[2-5]. Thus the study of EOT of a metallic film with subwavelength holes has attracted much attention. Numerous researchers have designed various subwavelength nanoholes with different topologic shapes to enhance transmittance and explore underlying physical mechanisms^[6-21].

Originally, it is widely believed that the EOT phenomenon can be mainly attributed to surface plasmon polaritons (SPPs). They are surface electromagnetic waves of collective electron oscillations induced by the coupling of light with surface charges under the Bragg coupling condition^[6]

$$\operatorname{Re}\left[\frac{\omega}{c}\sqrt{\frac{\varepsilon_m\varepsilon_d}{\varepsilon_m+\varepsilon_d}}\right]=|k_0\sin\alpha+iG_x+jG_y| \quad (1)$$

where w , c , ε_d , ε_m , k_0 , α , and (i,j) are the angular frequency, light speed, the relative permittivity of the dielectric material, the relative permittivity of the metal, the momentum of free-space light, the incident angle, and the order of specific SPP modes, respectively. In addition, the optical transmission process through the metallic holes includes multiple light diffractions. Bloch wave modes provide another understanding of the physics mechanism for EOT through their inherent coherent diffraction^[7].

Recently, it has been found that the localized surface plasmon (LSP) has the unique ability to overcome the diffraction limit, the minimum size, and the electric field constraint^[9]. Thus, the LSP of the sub-wavelength hole also plays an important role in the EOT phenomenon. It induces a strong EOT effect on metallic holes with highly acute angles^[9]. To better

understand the contribution of SPPs and LSP to the EOT phenomenon, researchers had fixed the shape and the size of hole and changed the period of the structure^[10]. Furthermore, the waveguided mode resonance that is similar to Fabry-Perot (FP) also enhances transmission in the slit because the slit can be considered as a metallic waveguide section, with both ends open to space^[11].

The results show that the resonant EOT phenomenon caused by LSP has narrow spectral bandwidth^[12-14]. Recently, the researchers have used the connection between larger rectangular apertures and smaller apertures^[15], metallic circular nanohole arrays^[16], and metallic gratings with tapered slits^[17] to achieve the EOT of broadband transmission. Subramania G et al^[15] pointed out that through the double-groove structure can realize the nonresonant broadband enhanced transmission, improving some disadvantages of broadband optical transmission enhancement phenomenon light by obliquely incident TM polarization, such as large angle oblique incidence of the lack of practicality. The larger aperture aids the coupling of the incoming light, while a significant fraction of the incident power is funneled through the smaller aperture. The non-resonant operation renders the proposed structure functional in a very broad wavelength range, starting from 3 μm and continuing well into far-IR wavelengths. Shen Honghui^[17] et al. pointed out that non-resonant broadband enhanced transmission can be achieved by metallic gratings device with linearly tapered slits. By gradually varying the impedance from input to output plane, and effectively destroy the FP type resonant conditions of guided modes in the slit, yield a non-resonant broadband and wide-angle large transmission in the infrared. In recent years, some researchers study the dependence of the transmission spectrum of slit on the depth of the embedded groove^[19]. Qin Y^[20] et al. had investigated the influence of the parameters of the rectangular cavity on the transmission of tapered metallic slits array. However, the influence of

parameters such as the slope of the slit, the thickness and period of the array on the structure transmission is not discussed^[18-20].

This study indicates that the tapered slits array embedded with rectangular cavity operating under normal incidence can also generate broadband transmission for TM polarized light. The electric field (E_y) distributions in this structure are analyzed. The simulation results show that the proposed structure not only possesses all the capabilities of EOT, but also achieves a nonresonant broadband enhanced transmission in infrared. In addition, the transmission properties are strongly dependent on structural parameters; therefore, these results can guide the design of near-field light harvesting devices with broadband and strong transmission capability. It can also improve understanding of the mechanisms of the extraordinary optical transmission phenomenon.

1 Structure and computational method

The schematic diagram of tapered slits array embedded with rectangular cavity is show in Fig.1. The grating is periodic in the x -direction. The tapered slits is characterized by the thickness H , period P , and widths W_{in} and W_{out} =30 nm at the entrance and exit of the slit, respectively. The parameters of the rectangular cavity is characterized by the length l , thickness t , and the position h . The position of the z -direction in the rectangular cavity h is defined as the distance between the bottom of the rectangular cavity and the exit of the slit. We assume surrounding, substrate, rectangular cavity and slit material to be air. As shown in Fig.1, the incident light is perpendicular to the incident direction of metal film, the incident polarization of x -direction (θ).

All transmission spectra were normalized by the incident light intensity. We define peak transmittance for short wavelength range and long wavelength range are T_{s-peak} and T_{l-peak} , respectively. The transmission coefficient is defined as the rate of output power P_{out} to input power P_{in} , namely, $T=P_{out}/P_{in}=|E_{tran}/E_{in}|^2$. The

calculated region is truncated by periodic boundary conditions along the x -direction and perfect matched layers along the z -direction. The silver(Ag) with good conductivity is employed in such a structure. The complex relative permittivity of Ag is obtained from Ref.[22-23].

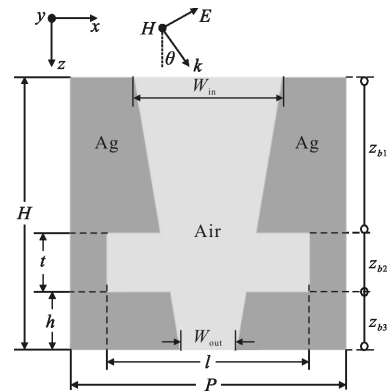


Fig.1 Schematic diagram of the metallic grating with tapered slits embedded with rectangular cavity

2 Numerical results and discussion

Firstly, to investigate the effect of entrance width W_{in} on the transmission property of the grating, W_{in} is increased from W_{in} =30 nm to W_{in} =390 nm, with fixed P =400 nm, H =400 nm, l =300 nm, t =90 nm, h =30 nm, and W_{out} =30 nm. As shown in Fig.2, the transmission peak are strongly affected by W_{in} . The blue-shift of transmission peak where W_{in} changes from 30 to 390 nm are observed in Fig.2, and the transmittance increases gradually at long wavelengths. Surprisingly, the transmission intensity increases from 42% to 94% , accompanied by an enhanced transmission band when W_{in} varies from 30 to 150 nm. The maximum transmission is up to 94% as W_{in} =150 nm. Based on the large transmission enhancement by tapering, the width of the entrance to the exit is smaller and smaller. We can imagine that the light is slowly squeezed from the entrance of the taper on to the narrower exit slit. Therefore, the field is expected to be gradually enhanced.

To confirm, we plot the electric field spatial distribution(Fig.3) at broadband transmission wavelength

$\lambda=6\ \mu\text{m}$ for tapered metallic slits array embedded with rectangular cavities corresponding to Fig.2. For other grating sizes, the field spatial distribution profiles are very similar. We notice indeed that the electric amplitude gradually increases towards the exit of the slit by tapered slits array, contrasting Fig.3(a)–(c). In addition, the fields reach their maximum exactly at the exit of the slits array, and the maximum value is much larger than in the straight metallic slits array case. For the whole tapered metal slits, the characteristic impedance is reduced from the entrance of the slit to the top surface of rectangular cavities, with the increase of the width of the entrance. So the total characteristic impedance of the structure is decreasing with the increase of W_{in} (more "open" gratings), and the long wavelength range of the transmittance increases.

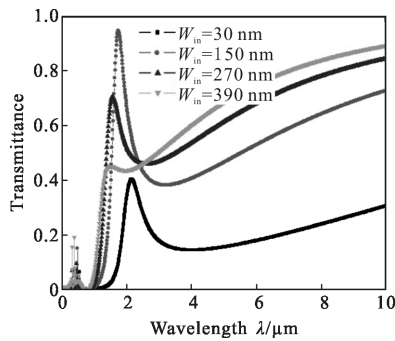


Fig.2 Calculated transmission spectra through tapered metallic slits array embedded with rectangular cavities with different widths W_{in}

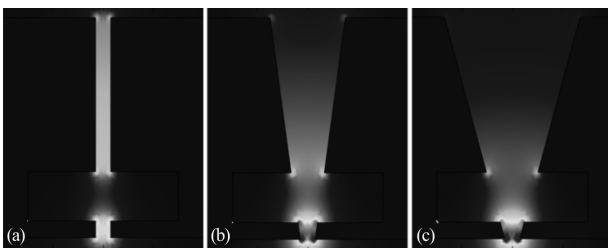


Fig.3 Electric field distributions at $\lambda=6\ \mu\text{m}$ for tapered metallic slits array embedded with rectangular cavities with (a) $W_{\text{in}}=30\ \text{nm}$, (b) $W_{\text{in}}=150\ \text{nm}$, (c) $W_{\text{in}}=270\ \text{nm}$

To examine the field enhancement properties, Fig.4 shows the average normalized electric field as a

function of wavelength at the slit exit (same gratings as in Fig.3). Broadband field enhancement is obtained, and it increases as the taper becomes wider (increasing W_{in}). Meanwhile, the spectrum of the normalized field is similar to the corresponding transmission spectrum (Fig.4). Therefore, the near-field at the exit of the slit and the transmission have a similar spectrum, with deviations from evanescent wave components. The average field decreases towards smaller wavelengths, since there is less light transmission. However, by tapering it is still possible to obtain a local field enhancement, instigated by the sharp corner at the exit of the slit, as the field maxima shown in Fig.4. Therefore, tapering offers a strong control over the field enhancement profile, by tailoring the transmission spectrum, the corner sharpness.

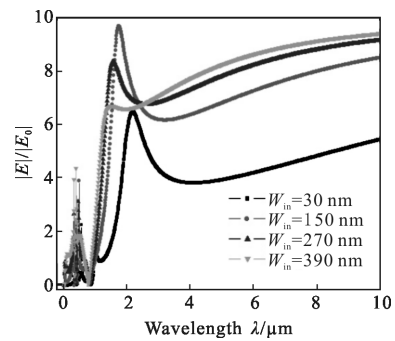


Fig.4 Average E field amplitude (normalized by the incident field amplitude E_0) versus wavelength at the exit of slit for gratings with different widths W_{in}

Figure 5 (a) plots the simulated transmission spectra of the tapered metallic slits array with different incidence angles θ of 0° , 20° , 40° , 60° and 80° . Other parameters in this structure are the same with those in Fig.3 ($W_{\text{in}}=150\ \text{nm}$). As is stated above, when $\theta=0^\circ$, there are obvious transmission peaks and broadband transmission. The transmission decreases with the increased of incidence angle, as shown in Fig.5 (a). Figure 5 (b) shows the polar plot of the transmittance of tapered metallic slits at $\lambda=6\ \mu\text{m}$. With different incident polarization angles, the maximum transmittance is found to occur at $\theta=0^\circ$ and $\theta=180^\circ$

as shown in Fig.5(b). This is similar to the transmission characteristics of the conventional subwavelength slit structures.

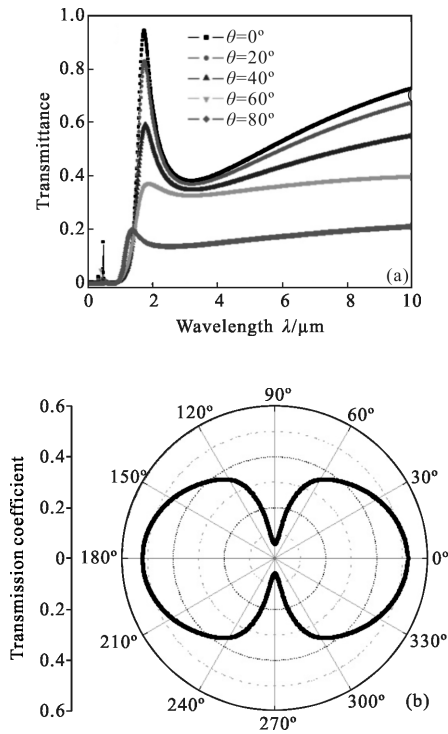


Fig.5 (a) Transmission spectra of tapered metallic slits array embedded with rectangular cavities with different incident polarization angle θ ; (b) Polar plot of the transmittance of tapered metallic slits array embedded with rectangular cavities at $\lambda=6 \mu\text{m}$ ($W_m=150 \text{ nm}$)

The tapered slits is composed of upper and lower monolayer slits that are separated by a long rectangular cavities. Each monolayer slit can be fabricated independently during experimentation. Hence, the centers of these slits may not be aligned. The transmission properties of the tapered slits as presented in Fig.6 (a). The no-naligned structures are fixed at $W_{in}=200 \text{ nm}$, $W_{out}=30 \text{ nm}$, $l=300 \text{ nm}$, $t=60 \text{ nm}$, $h=170 \text{ nm}$, $H=400 \text{ nm}$, and $P=400 \text{ nm}$. The deviation in the centers of the two monolayers is denoted by w . Although the transmission of short wavelength is increase as suggested in Fig.6(b), the transmittance does not vary obviously with w . The transmittance at the non-resonant broadband decreases slightly with the increase in w . The result exhibited in Fig.6 (b) imply

that the asymmetry and the smaller deviation of the two separated monolayers do not alter the performance of broadband, and the enhanced transmission of the tapered slits obviously in the infrared region. This finding can thus guide the fabrication of such slits and their future applications in near-field optics.

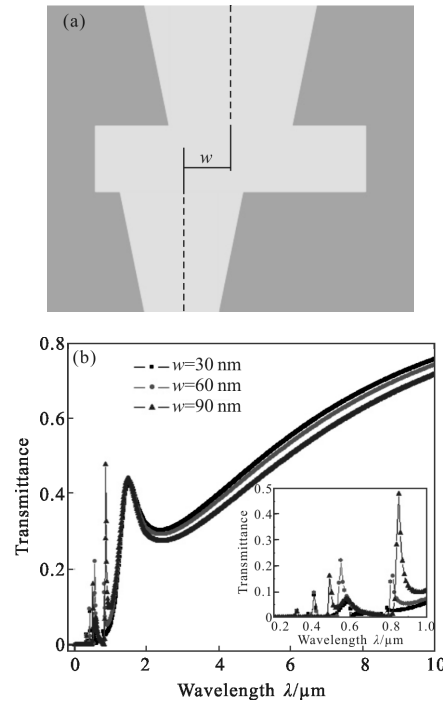


Fig.6 (a) Schematic of the taped slits in which the centers of two separated monolayer slits deviate; (b) Simulated transmission spectra of the tapered slits with different w values

3 Conclusion

This study proposed a paradigm structure of tapered slits array embedded with rectangular cavities to realize nonresonant broadband EOT. In the tapered slits array embedded with rectangular cavities, the transmission spectra are investigated using FEM. Results show that the transmission properties of the slits arrays strongly depend on incident polarization and structural parameters. When the rectangular cavity is embedded, the characteristic impedance of the slit is decreased, which is also the reason for the increase of transmission. In addition, increase in entrance width provides a strong enhancement and localization of light at the exit of the slit, used for applications such

as nonlinear optics and light harvesting. Finally, the effects of the centers misalignment of tapered slits structure on the transmission property are also studied.

References:

- [1] Ebbesen T W, Lezec H J, Ghaemi H F, et al. Extraordinary optical transmission through sub-wavelength hole arrays [J]. *Nature*, 1998, 391(6): 667–669.
- [2] Barnes W L, Dereux & Amp A, Ebbesen T W. Surface plasmon subwavelength optics.[J]. *Nature*, 2003, 424(6950): 824–830.
- [3] Sun Bin, Wang Lingling, Wang Liu, et al. Improved extraordinary optical transmission though single nano-slit by nano-defocusing. [J]. *Opt Laser Technol*, 2013, 54: 214 – 218.
- [4] Wijesinghe T M, Premaratne M, Agrawal G P. Low-loss dielectric-loaded graphene surface plasmon polariton waveguide basedbiochemical sensor [J]. *Journal of Applied Physics*, 2015, 117(21): 641–648.
- [5] Grodecki K, Bozek R, Strupinski W, et al. Raman spectroscopy on transition metals [J]. *Analytical & Bioanalytical Chemistry*, 2007, 388(1): 29–45.
- [6] Ortuno R, Garcíaameca C, Rodríguezfortuno F J, et al. Modeling high-order plasmon resonances of a U-shaped nanowire used to build a negative-index metamaterial [J]. *Physical Review B*, 2009, 79(7): 075103.
- [7] Delgado V, Marqués R. Surface impedance model for extraordinary transmission in 1D metallic and dielectric screens[J]. *Optics Express*, 2011, 19(25): 25290–25297.
- [8] Fang Junfei, Deng Jianping, Zhang Pengchao. Enhancement of radiative properties of silver by surface structure with spherical resonant cavity [J]. *Infrared and Laser Engineering*, 2016, 45(9): 0916001. (in Chinese)
- [9] Rodrigo S G, Mahboub O, Degiron A, et al. Holes with very acute angles: a new paradigm of extraordinary optical transmission through strongly localized modes [J]. *Optics Express*, 2010, 18(23): 23691–23697.
- [10] Yao Chenggang, Li Jun, Li Long. Structural optimization of ring resonant cavity consisted with symmetry prisms [J]. *Infrared and Laser Engineering*, 2016, 45 (11): 1118002. (in Chinese)
- [11] Chen J, Li Z, Lei M, et al. Broadband unidirectional generation of surface plasmon polaritons with dielectric film coated asymmetric single slit [J]. *Optics Express*, 2011, 19 (27): 26463–26469.
- [12] Marani R, Marrocco V, Grande M, et al. Enhancement of extraordinary optical transmission in a double heterostructure plasmonic bandgap cavity[J]. *Plasmonics*, 2011, 6(3): 469–476.
- [13] Hou Y. Extremely high transmittance at visible wavelength induced by magnetic resonance [J]. *Plasmonics*, 2011, 6(2): 289–293.
- [14] Liu Jianping, Wang Lingling, Sun Bin, et al. Enhanced optical transmission through a nano-slit based on a dipole source and an annular nano-cavity [J]. *Opt Laser Technol*, 2015, 69: 71–76.
- [15] Subramania G, Foteinopoulou S, Brener I. Nonresonant broadband funneling of light via ultrasubwavelength channels [J]. *Physical Review Letters*, 2011, 107(16): 163902.
- [16] Pang S, Zhang Z, Qu S. Nonresonant enhanced optical transmission through the metallic circular nanohole arrays[J]. *Scientia Sinica*, 2014, 44(2): 142–149. (in Chinese)
- [17] Shen H, Maes B. Enhanced optical transmission through tapered metallic gratings [J]. *Applied Physics Letters*, 2012, 100(24): 241104.
- [18] Nooshnab V, Golmohammadi S. Revealing the effect of plasmon transmutation on charge transfer plasmons in substrate-mediated metalodielectric aluminum clusters [J]. *Optics Communications*, 2017, 382: 354–360.
- [19] Li Yihan, Zhang Mile, Cui Hailin, et al. Terahertz absorbing properties of different metal split-ring resonators[J]. *Infrared and Laser Engineering*, 2016, 45(12): 1225002. (in Chinese)
- [20] Qin Y, Cao W, Zhang Z Y. Enhanced optical transmission through metallic slits embedded with rectangular cavities[J]. *Acta Physica Sinica*, 2013, 62(12): 127302. (in Chinese)
- [21] Alù A, D' Aguanno G, Mattiucci N, et al. Plasmonic Brewster angle: broadband extraordinary transmission through optical gratings [J]. *Physical Review Letters*, 2011, 106(12): 123902.
- [22] Economou E N. Surface plasmons in thin films [J]. *Physical Review*, 1969, 182(2): 539–554.
- [23] Palik E D. Lithium Niobate (LiNbO₃) [J]. *Handbook of Optical Constants of Solids*, 1997, 20(2): 695–702.